ELSEVIER

Biochimica et Biophysica Acta 1280 (1996) 223–230

BBA Biochimica et Biophysica Acta

Comparison of photosensitized plasma membrane damage caused by singlet oxygen and free radicals

Irene E. Kochevar *, Christopher R. Lambert, Mary C. Lynch, Antonio C. Tedesco [1]

Wellman Laboratories of Photomedicine, Department of Dermatology, Massachusetts General Hospital, Harvard Medical School, Boston, MA 02114, USA

Received 13 July 1995; revised 17 November 1995; accepted 4 December 1995

Abstract

The efficiency and selectivity of photosensitized damage to membrane functions may be influenced strongly by the identity of the initial reactive species formed by the photosensitizer. To test this possibility, a photosensitizer, rose bengal (RB), was used that resides in the plasma membrane and which generates singlet molecular oxygen ($^1O_2^*$) upon excitation with visible light, and radicals plus $^1O_2^*$ upon excitation with UV radiation. With this approach, $^1O_2^*$ and radicals are formed at the same locations in the plasma membrane. The response of three plasma membrane functions, namely, proline transport, membrane potential, and membrane impermeability to charged dye molecules, was assessed. The efficiencies of the responses in the presence and absence of oxygen were compared per photon absorbed by RB at two wavelengths, 355 nm (UV excitation) and 532 nm (visible excitation). The efficiency of oxygen removal before irradiation was assessed by measuring the RB triplet lifetime. The three membrane functions were inhibited more efficiently at 355 nm than at 532 nm in the presence of oxygen indicating that the radicals are more effective at initiating damage to membrane components than $^1O_2^*$. The ratio of photosensitized effects at the two wavelengths in the presence of oxygen was the same for two membrane functions but not for the third suggesting that $^1O_2^*$ and radicals initiate a common mechanistic pathway for damage to some membrane functions but not to others. Removing oxygen reduced the efficiency of 355 nm-induced photosensitization by factors of 1.4 to 7. The sensitivity of the three membrane functions to $^1O_2^*$-initiated damage varied over a factor of 50 whereas radical initiated damage only varied by a factor of 15. In summary, these results indicate that radicals and $^1O_2^*$ formed at the same locations in the plasma membrane vary in their efficiency and specificity for membrane damage but may, in some cases, operate by a common secondary damage mechanism in the presence of oxygen.

Keywords: Photosensitization; Singlet oxygen; Free radical; Plasma membrane; Photodynamic therapy; Membrane potential; Proline transport; Lipid oxidation

1. Introduction

Photosensitization in biology is the process in which a molecule, termed the photosensitizer, absorbs visible or ultraviolet energy and subsequently produces reactive species that alter cellular molecules and initiate cellular responses. Therapeutic applications of light-induced cytotoxicity, especially for destruction of tumor tissue (photodynamic therapy), have increased recently because improved photosensitizers and light delivery systems have been developed [1–3]. Other promising medical applications of photosensitization are purging of bone marrow of leukemic cells for transplantation and elimination of viruses from blood components for transfusions [4,5].

Applications of photosensitization as a tool in biology include targeting cell populations such as specific neurons [6,7] and cells that are actively endocytosing [8,9]. Dyes plus photoirradiation have been used to generate specific reactive oxygen species as an aid to understanding mechanisms in reperfusion injury [10,11] and to cause focal thrombosis [12,13]. Subcellular sites have been targeted using a dye attached to monoclonal antibodies and pulsed laser irradiation [14–16]. Applications of photosensitization in medicine and biology would benefit from greater efficiency and greater selectivity for targeting cellular and subcellular sites.

Abbreviations: HBSS, Hanks' balanced salt solution; RB, rose bengal; $^1O_2^*$, singlet molecular oxygen; bis-oxonol, bis-(1,3-diethylthiobarbituric acid)trimethine oxonol.

* Corresponding author. Fax: +1 (617) 7263192; e-mail: kochevar@helix.mgh.harvard.edu.

[1] Permanent address: Faculdade de Filosofia, Ciências e Letras de Ribeirão Preto, Universidade de São Paulo, Ribeirão Preto, SP, Brazil.

SSDI 0005-2736(95)00297-9

Many of the photosensitizers used in biology and medicine localize in cellular membranes, either the plasma membrane or intracellular membranes. In general, the reactive species produced diffuse only very short distances before reacting [17,18]; thus, the initial damage is limited to sites close to the photosensitizer. Membrane photosensitization has been shown to decrease the plasma membrane potential [19–21], inhibit transport of molecules across the plasma membrane [22,23], and both inhibit and activate membrane associated enzymes [24,25]. Cellular responses induced by plasma membrane photosensitization include apoptosis [26] and expression of early response genes [27].

The primary step in photosensitization is the formation of reactive species. Many photosensitizers produce singlet oxygen ($^1O_2^*$), a highly reactive excited state of oxygen, by energy transfer from the excited triplet state of the photosensitizer. Another primary reaction is the formation of free radicals from the photosensitizer either through cleavage of weak bonds in the photosensitizer or electron transfer reactions. The reactions of $^1O_2^*$ and free radicals with unsaturated lipids and proteins in the membrane may directly cause alterations in membrane functions.

A major goal of this study was to generate $^1O_2^*$ and free radicals at the same sites in the plasma membrane and determine whether these species are equally efficient and selective toward membrane components. The approach used was to hold the location for formation of reactive species constant by using a single photosensitizer and to vary the reactive species by choosing a photosensitizer that produces different reactive species under different irradiation conditions. Our recent results [21] indicate that the location of $^1O_2^*$ formation in the plasma membrane strongly influences the relative damage to different membrane components. The responses of three membrane functions to photosensitization were determined in this study. If the identity of the primary reactive species strongly influences the membrane damage, the relative effect on these membrane functions should vary with the reactive species produced. Alternatively, if damage to membrane functions results mainly from a subsequent mechanism, such as lipid oxidation, the relative effect on the membrane functions should not vary greatly with the reactive species produced. Rose bengal (RB) was chosen as the photosensitizer because our previous studies demonstrated that $^1O_2^*$ is generated upon excitation with visible radiation and highly reactive radicals are produced, in addition to $^1O_2^*$, on excitation with UV radiation [28].

2. Materials and methods

2.1. Chemicals

Rose bengal was obtained from Aldrich (Milwaukee, WI) with a stated purity of 97% and used as received. Hanks' balanced salt solution (HBSS), Hepes buffer (20 mM *N*-(2-hydroxyethyl)piperazine-*N'*-(2-ethane sulfonic acid), pH 7.4), trypan blue and cell culture media were obtained from Gibco BRL Products (Life Technologies, Gaithersburg, MD). Bis-(1,3-diethylthiobarbituric acid)trimethine oxonol (bis-oxonol) was obtained from Molecular Probes (Eugene OR) and L-[^{3}H]proline from Amersham (Arlington Heights, IL). Nitrogen (99.8%) was obtained from Airco Industrial Gases (Kittery, ME). An RB stock solution (500 μM) was prepared in 5 mM phosphate-buffered saline (pH 7.4), divided into 0.5 ml aliquots and stored at −20°C. The stock solution was diluted to a final concentration of 3 μM in the cell suspension.

2.2. Cell culture

P388D$_1$ cells, a mouse macrophage monocyte line that grows in semi-suspension, was obtained from the American Type Culture Collection (ATCC No. CCL46). Cells were cultured in Fischer's media supplemented with 10% heat inactivated horse serum in 175 cm^2 culture flasks at 37°C with 5% CO_2. The day before an experiment, cells were seeded at $0.3 \cdot 10^6$ cells/ml.

2.3. Absorbance measurements

Cells were incubated with 3 μM RB in HBSS for 20 min, centrifuged and the absorbance of the supernatant at the maximum near 550 nm was determined to measure the uptake of RB by cells following the procedure described previously [21]. In a separate experiment, the absorbance at the irradiation wavelengths, 355 and 532 nm, were measured on a cell suspension ($1 \cdot 10^6$ cells/ml) containing 3 μM RB using a cell suspension without RB as the reference.

2.4. Irradiations

Prior to irradiations cells were harvested, washed twice in HBSS (pH 7.4) and resuspended at $1 \cdot 10^6$ cells/ml in HBSS. When required, N_2-gassing was performed as described below. The cells were stirred slowly with a micro stirring bar during the irradiation in a 1 cm path length quartz cuvette; the sample volume was 1.2 ml. All samples, including non-irradiated controls were stirred for the same length of time in a given experiment. Control samples for all experiments included cells treated with RB but not irradiated, and cells not treated with RB but exposed to the highest light dose.

Irradiations employed a Quantel YG 660A Q-switched Nd:YAG laser (Continuum, Santa Clara, CA) either frequency doubled to produce 532 nm or frequency tripled to produce 355 nm radiation. The pulse length was 8 ns, the beam diameter incident on the sample was 6 mm and the repetition rate was 5 Hz. The pulse energy was typically 10 mJ as measured with a Scientech (Boulder, CO) disc calorimeter (type 38-0101) with a Scientech digital indica-

tor (type 365). The maximum irradiation time was 3 min 40 s. The laser energy was monitored continuously during the course of an experiment. Under these conditions, the laser pulse intensity at both wavelengths was $4.4 \cdot 10^6$ W/cm^2. For experiments measuring membrane potential, very low total doses were used. In this case, the pulse energy was lowered to 3 mJ in order to deliver enough pulses to irradiate the sample evenly. Variable numbers of pulses were used to deliver each specified dose.

2.5. Reduction of oxygen concentration in cell suspensions

The oxygen content of certain samples was reduced by N_2 saturation. Samples were placed in fluorescence cuvettes and sealed with a rubber septum. Nitrogen was blown gently over the surface of the stirred sample for 40 min. Control experiments showed that this treatment did not adversely affect the membrane functions studied compared to air-saturated samples. The sample contained RB during this procedure except for the proline transport experiments where an aliquot of N_2-gassed stock RB solution was injected 20 min before completion of the nitrogen gassing procedure. Unirradiated control samples taken at the beginning and end of each experiment and treated in the same way as irradiated samples showed that the cells had not deteriorated during the course of the experiment.

To determine whether each cell suspension containing RB was thoroughly deoxygenated by the N_2 gassing procedure, the lifetime of the RB triplet was determined using laser flash photolysis before irradiation. The laser flash photolysis apparatus has been described previously [29]. The same laser was used for the laser flash photolysis as for the irradiations. Control experiments showed that the monitoring lamp and the single laser pulse used to acquire the RB triplet kinetics by laser flash photolysis did not produce photodamage to any of the membrane functions assayed. Rose bengal was excited at 532 nm or 355 nm and time-resolved absorption changes monitored at 520 nm, a wavelength where a large difference absorption (typically $2 \cdot 10^{-2}$ M^{-1} cm^{-1}) can be detected. In an air-saturated cell suspension, the lifetime of RB triplet was ~ 2 μs. The N_2 gassing procedure increased the RB triplet lifetime to > 60 μs indicating that the oxygen concentration was lowered significantly. Under these conditions, irradiation at 532 nm of samples having RB triplet lifetimes of > 60 μs did not produce alterations to any of the membrane functions at light doses which caused significant damage in the air-saturated samples. The RB triplet lifetime was measured on all N_2-gassed cell suspensions before irradiation at either 355 or 532 nm. Only samples having RB triplet lifetimes > 60 μs were used.

2.6. Plasma membrane potential assay

Our previous procedure was modified for this study [21]. For each light dose, 3 samples (1.2 ml each), were irradiated, placed on ice immediately, and kept in the dark until the beginning of the assay. When all the irradiations were complete, the 3 samples were combined (3.6 ml total) and washed three times with cold Hepes buffer to reduce the amount of RB present. The pooled sample was then assayed as three 1.2 ml aliquots. Each was transferred to a fluorescence cuvette and maintained at 37°C for 10 min to equilibrate to temperature. The fluorescence of residual RB ($\lambda_{ex} = 540$ nm, $\lambda_{em} = 565$ nm) was measured on this sample. This value was subtracted from all subsequent measurements of bis-oxonol fluorescence; it was always less than 10% of the total fluorescence intensity. An aliquot (6 μl) of the fluorescent probe dye, bis-oxonol, was added from a 150 μM stock solution to give a final concentration of 0.75 μM. After incubation at 37°C for a further 10 min, the intensity of the fluorescence was measured ($\lambda_{ex} = 540$ nm, $\lambda_{em} = 565$ nm). The cells were completely depolarized by adding 48 μl KCl (4 M), incubating 10 min, and 4 μl gramicidin (2 mg/ml) and incubating the sample at 37°C for a further 10 min; the fluorescence of this sample was then measured. The relative polarization of the sample was determined from the formula,

$$\text{Fraction membrane potential} = \frac{F'_{dp} - F_{exp}}{F_{dp} - F_o}$$

where F_o is the fluorescence intensity of bis-oxonol in an unirradiated sample, F_{exp} is the fluorescence of bis-oxonol in an irradiated sample, F_{dp} is the fluorescence of bis-oxonol in a fully depolarized, unirradiated sample and F'_{dp} is the fluorescence of bis-oxonol in a fully depolarized irradiated sample. Because sample preparation caused a variable amount of depolarization, the maximum depolarization achievable by addition of KCl and gramicidin was measured before each experiment. Preparations were only used if at least a 60% change in fluorescence was obtained. The standard deviation on the triplicate measurements was typically $\pm 15\%$ of the mean. Unirradiated control samples were treated in the same manner as irradiated samples for each set of experiments.

2.7. Proline transport assay

The procedure used previously [21] was adapted to samples containing only $1 \cdot 10^6$ cells/ml. Three 1.2 ml samples were irradiated at each delivered light dose. Immediately following irradiations, the three samples were combined and stored on ice. For analysis, the combined sample was centrifuged and resuspended in 2.4 ml of ice-cold HBSS to produce a final concentration of $1.5 \cdot 10^6$ cell/ml. Prior to being assayed, the sample and the proline mixture were incubated separately at 37°C for 10 min to allow the temperature to equilibrate. At this time the inner stores of amino acids in the cells were depleted having been in HBSS for at least 1 h. A 184 μl aliquot of the

proline mixture was then added to 800 μl of sample; the final concentrations were 12.3 μCi/assay of L-[^{3}H]proline and 18.8 μM unlabeled L-proline. The mixture was shaken gently and maintained at 37°C for 4 min, a time shown in preliminary experiments to be in the linear portion of the uptake curve. At the end of this time, 10 ml of ice-cold HBSS was added and the sample kept on ice until all the assays were complete. The samples were centrifuged for 6 min in the cold (300 × *g*; Sorvall Model RT6000 centrifuge), and the supernatant decanted. The sample was washed three times with ice-cold HBSS. The tip of the centrifuge tube containing the cell pellet was cut off and added to 3.5 ml of scintillation fluid (Liquiscint, National Diagnostics) in a scintillation vial. The samples were shaken and counted using a Beckman LS3801 liquid scintillation counter. Three assays were carried out on each 2.4 ml sample. Standard deviations for the triplicate measurements were typically ±30% of the mean.

2.8. Membrane permeability assay

Following irradiation the cell suspension was allowed to stand for 1 h ± 5 min at room temperature in the dark. A 100 μl aliquot was diluted 1:1 with a 0.4% trypan blue solution and two chambers in a hemacytometer were counted immediately. A minimum of 50 cells were counted for each assay. The range of the duplicate determinations was typically ±15% of the average.

3. Results

3.1. Uptake of RB by cells

The uptake of RB by cells was determined by incubating cells with 3 μM RB for 20 min, centrifuging and comparing the absorbance of the supernatant with the absorbance of a cell-free RB sample. These measurements indicated that 72% of the RB was associated with cells at $1 \cdot 10^6$ cells/ml. This value was used to calculate the fraction of light that was absorbed by RB in the plasma membrane.

3.2. Absorption of 355 nm and 532 nm light by RB in cell membranes

The absorption spectrum of 3 μM RB in cell suspension ($1 \cdot 10^6$ cells/ml) against a cell suspension reference is shown in Fig. 1. In order to compare the efficiency of photosensitization at 355 and 532 nm, the number of photons absorbed for each incident light dose must be known. The absorbance of a sample containing 3 μM RB and $1 \cdot 10^6$ cells/ml was 0.12 at 532 nm and 0.01 at 355 nm, using a cell suspension without RB as the reference. Using these values and considering that 72% of the RB molecules are associated with the cells, the percent of the incident light absorbed by membrane-bound RB is calculated to be 18% at 532 nm and 1.6% at 355 nm. Because the visible absorption maximum of RB in membranes red-shifts slightly [30], the percent light absorbed at 532 nm may be slightly lower than this value; the value for 355 nm should be unaffected since the absorbance does not vary greatly with wavelength in this region of the spectrum. The absorbed doses of radiation at the two wavelengths were converted into numbers of photons absorbed by multiplying by the number of photons/joule at each wavelength.

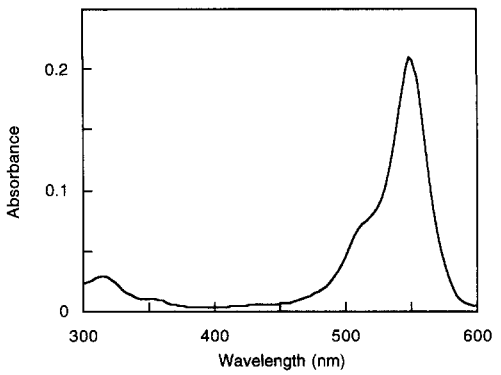

Fig. 1. Absorption spectrum of 3 μM rose bengal in P388D$_1$ cell suspensions ($1 \cdot 10^6$ cells/ml) in Hanks' balanced salt solution. Reference sample contained cell suspension alone.

3.3. Photosensitized depolarization of the plasma membrane

The plasma membrane potential was monitored using the fluorescence of bis-oxonol [19,21]. Potential interference from RB fluorescence in the measurement of bis-oxonol emission was minimized by washing the cells twice before determinations. Residual rose bengal fluorescence, typically 10% of the bis-oxonol fluorescence, was measured for all samples prior to the addition of the bis-oxonol. Treatment with RB in the dark or with the highest light dose (355 nm or 532 nm) in the absence of RB did not decrease the membrane polarization. The results were expressed as the fraction of membrane potential compared to the RB-treated, unirradiated controls in order to normalize results from different experiments and plotted versus photons absorbed by membrane-bound RB (Fig. 2).

To compare the efficiency of photosensitization under different conditions and for different membrane functions, the number of photons absorbed by membrane-bound RB that causes a 50% change in the membrane function was defined as the P_{50} value. Each P_{50} value was calculated from the equation for the exponential fit of the data. The lower the P_{50} value, the more efficient the photosensitization process. To calculate the error associated with each P_{50} value, the difference between each measured value for a membrane function and the value from the fit curve was determined and the average percent difference calculated.

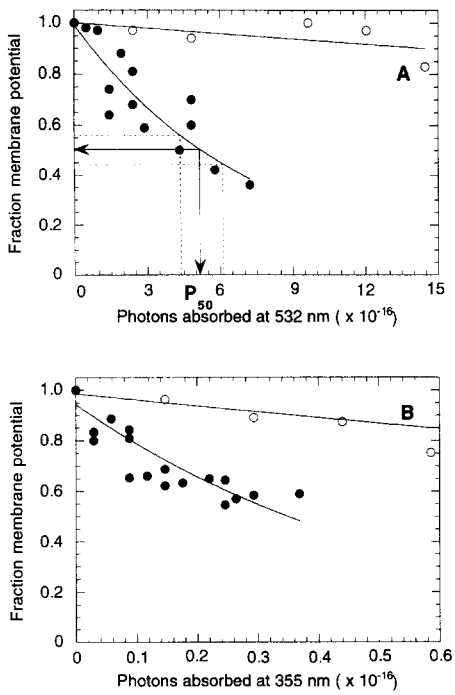

Fig. 2. Depolarization of the plasma membrane photosensitized by 3 μM rose bengal in the presence and absence of oxygen. Panel A shows results using 532 nm radiation. Panel B shows results using 355 nm radiation. Filled circles = aerated samples; open circles = N_2-gassed samples. Data are from at least two experiments for each aerated treatment and from a single experiment for N_2-gassed samples. The standard deviation of triplicate measurements for each treatment was typically 15% of the value.

This error on the y-axis is shown as the dashed horizontal lines extending to the fit curve in Fig. 2. The x-axis values for the intersection of these lines with the fit curve gave the errors in P_{50} (in photons absorbed on the x-axis) and are shown as the dashed vertical lines in Fig. 2. The P_{50} values, the error ranges and the correlation coefficient for each fit are given in Table 1.

Irradiation at 532 nm in the presence of oxygen caused significant loss of membrane polarization whereas in the absence of oxygen, photosensitized depolarization did not occur (Fig. 2A). When 355 nm radiation was used, the photosensitization efficiency increased; the P_{50} value in aerated samples was a factor of ~ 16 lower using 355 nm than using 532 nm radiation (Fig. 2). Oxygen depletion only partially inhibited the RB-photosensitized depolarization upon 355 nm irradiation as shown in Fig. 2B; at the maximum energy used, $1.2 \cdot 10^{16}$ photons, a 38% decrease in membrane potential was observed (data not shown). The P_{50} value was a factor of about seven larger in the air-saturated cell suspension.

3.4. Photosensitized inhibition of proline transport

The uptake of proline by cells was measured four min after mixing the cells with L-[^{3}H]proline. Experiments using control, unirradiated cells ($1 \cdot 10^6$ cells/ml) demonstrated that 4 min is in the linear portion of the uptake curve, similar to the results of previous studies [21]. The results are expressed as fraction of proline uptake compared to the RB-treated, unirradiated controls. Results from at least two experiments obtained with each irradiation condition are shown in Fig. 3 along with the curves showing the exponential fit of the data; correlation coefficients for the fits were > 0.91.

Irradiation of cell suspensions with 532 nm light in the presence of RB produced dose-dependent inhibition of L-[^{3}H]proline uptake in air-saturated samples but not in N_2-saturated samples, as expected for a $^1O_2^*$-mediated mechanism (Fig. 3A). Photosensitized inhibition of proline transport in air-saturated suspensions was approximately 6-fold more efficient using 355 nm than 532 nm radiation (Table 1). Removal of oxygen completely eliminated the photosensitized inhibition of proline using 532 nm radiation (Fig. 3A). In contrast, the presence of oxygen had virtually no effect on RB photosensitization induced by 355 nm radiation (Fig. 3B); the P_{50} values were the same within experimental error. Light alone (355 or 532 nm) at the highest doses used did not inhibit proline transport. Prolonged incubation (> 40 min) with RB alone caused inhibition of proline uptake in the dark in both N_2- and

Table 1
Efficiency of photosensitized alterations in plasma membrane functions using 3 μM rose bengal

Membrane function	P_{50} values, photons $\times 10^{-16}$ [a,b]			
	532 nm		355 nm	
	air	nitrogen [c]	air	nitrogen
Membrane potential	5.2 (4.4–6.1) [0.91]	–	0.35 (0.31–0.40) [0.93]	2.7 (2.5–2.9) [0.89]
Proline transport	19 (12–28) [0.96]	–	3.7 (2.9–4.7) [0.94]	2.6 (1.5–4.1) [0.91]
Membrane permeability	270 (230–320) [0.94]	–	16 (14–18)	41 (32–49)

[a] Mean value. Range given in parentheses was calculated from % error in measurements of membrane function as described in the text.
[b] Correlation coefficients for each fit are given in square brackets.
[c] Slopes of plots of fraction membrane function versus absorbed photons were all within experimental error of zero.

air-saturated cell suspensions. To avoid this effect, 20 min incubations were used for air-saturated samples and N_2-gassed stock RB solution was injected into the N_2-gassed (20 min) cell suspension and N_2-gassing was continued for 20 min. Control experiments showed that gassing RB-containing samples with air or N_2 for 20 min did not inhibit proline uptake. This procedure was not necessary for samples assayed for other membrane functions; only proline transport was sensitive to prolonged incubation with RB.

3.5. Photosensitized change in membrane permeability

The fraction of P388D$_1$ cells that stained with trypan blue was determined 1 h following irradiation and was used to monitor membrane permeability. Less than 5% of untreated cells were stained by trypan blue; neither the highest light doses in the absence of RB, nor RB treatment without light increased the trypan blue uptake. Nitrogen saturation completely inhibited the permeability induced by RB photosensitization using 532 nm excitation (Fig. 4A). The results obtained with 355 nm excitation did not show a simple exponential dependence on absorbed dose (Fig. 4B) in contrast to the results obtained for all of the other treatments and membrane functions. The line drawn in Fig. 4B is the fit to a second order polynomial equation suggesting a shoulder in the dose–response curve. Because these data could not be fitted to an exponential function no correlation coefficient is given. The P_{50} values indicate that nitrogen saturation decreases the efficiency of RB photosensitization upon 355 nm irradiation by a factor of approximately 2.5. Photosensitization by RB in air-saturated cell suspensions was approximately 17-fold more efficient using 355 nm than using 532 nm radiation (Table 1).

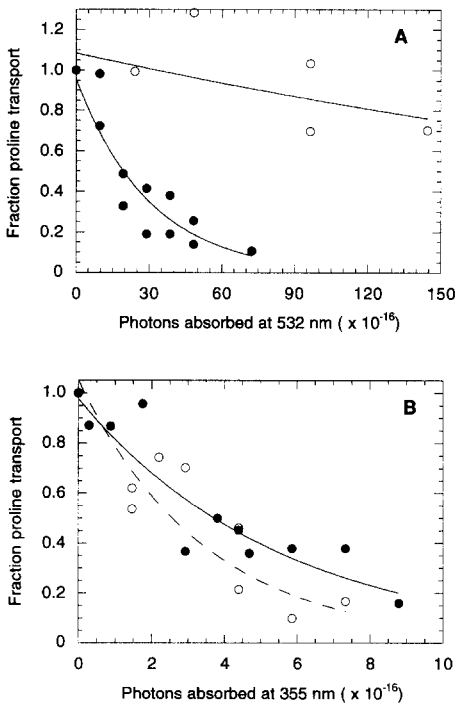

Fig. 3. Inhibition of proline transport by P388D$_1$ cells photosensitized by 3 μM rose bengal in the presence and absence of oxygen. Panel A shows results using 532 nm radiation. Panel B shows results using 355 nm radiation. Filled circles = aerated samples; open circles = N_2-gassed samples. Data from at least two experiments for each treatment condition were normalized to unity for the unirradiated, RB-containing control sample. The data points are the mean of triplicate measurements of a sample. The standard deviation on triplicate measurements for each treatment was typically 30% of the value.

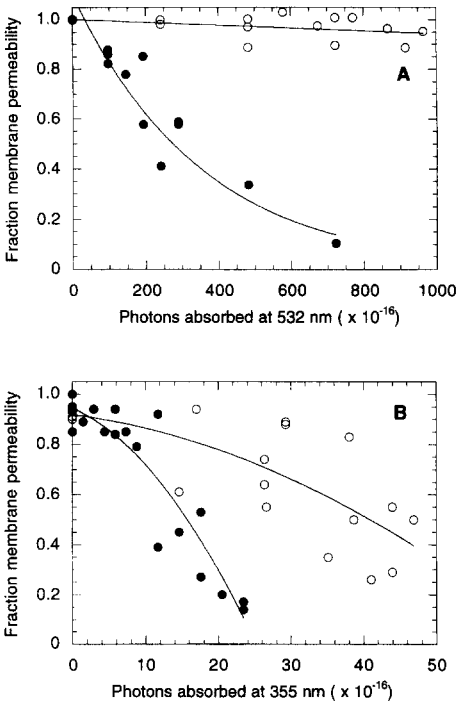

Fig. 4. Photosensitization of increased permeability of cells to trypan blue by 3 μM rose bengal in the presence and absence of oxygen. Panel A shows results using 532 nm radiation. Panel B shows results using 355 nm radiation. Filled circles = aerated samples; open circles = N_2-gassed samples. Data are from at least three experiments for each treatment condition and represent duplicate determinations on each sample.

4. Discussion

The approach taken to investigate the importance of the primary reactive species in membrane photosensitization was to use a single photosensitizer that produces different reactive species when excited at two different wavelengths. The two types of reactive species are generated at the same sites; use of two photosensitizers that generate different reactive species is complicated by differing locations of the two photosensitizers. Rose bengal was chosen because it displays wavelength dependent photochemistry [28] and resides in the plasma membrane. Although RB may eventually be at least partially internalized, the short period of incubation of cells with RB used in these experiments

minimizes this possibility. The structures of the radicals produced from irradiation of RB at 355 nm have not been characterized chemically. Our previous results indicated that carbon-iodine bond cleavage occurred which results in an iodine radical and a carbon-centered radical on the xanthene moiety. These radicals have not been identified spectroscopically and other radicals may form such as the RB cation radical from photoionization at 355 nm. Thus, the general term 'radicals' is used.

The first question asked was whether the radicals produced upon 355 nm excitation of RB in the presence of oxygen contribute to the damaging of membrane functions. If these radicals are not effective, equal P_{50} values are expected upon 532 and 355 nm excitation for each membrane function since equivalent yields of $^1O_2^*$ are formed at both wavelengths [28]. The results in Table 1 show that the P_{50} values are significantly lower at 355 nm than at 532 nm in air-saturated cell suspensions for all three of the membrane functions. This indicates that an efficient (radical-initiated) damage mechanism becomes very important and dominates the $^1O_2^*$ mechanism at the shorter wavelength. This result is consistent with findings of our previous study using RB solubilized together with acetylcholinesterase which showed that radicals were produced by 313 nm radiation with a quantum yield of ~ 0.001 and were about 200-times more effective than $^1O_2^*$ for enzyme inhibition [28]. The low efficiency of the $^1O_2^*$-mediated pathway relative to the radical-mediated pathway may result from the high rate of escape of $^1O_2^*$ from membranes [17].

A goal of this study was to determine whether $^1O_2^*$ and radicals cause damage to membrane components by discrete primary reaction mechanisms or cause damage by a shared secondary mechanism in the presence of oxygen. The results in Table 1 can be used to differentiate between these two possibilities. If a shared secondary mechanism for damage makes a major contribution to the photosensitization process in the presence of oxygen, the efficiency upon 355 nm excitation (where $^1O_2^*$ and radicals are both produced) should be greater than the efficiency upon 532 nm excitation ($^1O_2^*$ only) by the same factor for each membrane function, i.e., the ratio, $P_{50}(532)/P_{50}(355)$, should be the same for all three membrane functions. This ratio, $P_{50}(532)/P_{50}(355)$, was 15 for membrane potential, 5 for proline transport and 17 for membrane permeability. Thus, it appears that at least for some membrane functions (membrane potential and membrane permeability in these studies) a shared secondary mechanism dominates the processes leading to photosensitized damage initiated by $^1O_2^*$ and radicals. Since our previous results indicated that photosensitized damage occurs relatively close to the location of the photosensitizer [21], it appears even the secondary mechanism does not allow the reactive species to 'travel' far in the membrane.

For proline transport, the $P_{50}(532)/P_{50}(355)$ ratio in aerated samples was 5, much lower than for the other two membrane functions suggesting that the primary radicals produced upon 355 nm irradiation are more damaging that the secondary reactive species for this membrane function. The observation that the P_{50} values for proline transport were the same in the presence and absence of oxygen upon 355 nm irradiation also suggests that the radicals formed dominate the photosensitization mechanism and that a secondary process does not make a major contribution in the presence of oxygen (Table 1).

The results obtained in this study were also used to address the question of the relative selectivity of $^1O_2^*$ and radicals toward the membrane components controlling the three membrane functions. Because the efficiency for radical production from RB upon 355 nm excitation is not known in the plasma membrane, the relative ability of $^1O_2^*$ and radical molecules to cause damage cannot be quantitated. Under conditions where only $^1O_2^*$ is produced (532 nm irradiation, air-saturated), the P_{50} values for alterations in membrane potential, proline transport and membrane permeability varied over a range of 50. In contrast, when only radicals are produced (355 nm excitation, N_2-saturated) the range was only 15. These values indicate that the radical-initiated mechanism (in the absence of oxygen) is less selective than the $^1O_2^*$-initiated damage mechanism.

The photosensitization mechanism initiated by radicals in the presence of oxygen appears to involve an oxidative component for two of the three membrane functions. Comparison of the P_{50} values obtained upon 355 nm excitation indicates that for membrane potential and membrane permeability, the sensitization is significantly more effective in the presence than in the absence of oxygen although for proline transport, as noted above, the P_{50} values are the same within experimental error in air- and N_2-saturated samples. Since $^1O_2^*$ does not make a major contribution to the photosensitization at 355 nm excitation, it appears that a free radical initiated oxidative mechanism occurs.

The results in this study extend our previous work on membrane photosensitization with RB in which it was demonstrated that the location of a photosensitizer in the plasma membrane influences the relative damage to different membrane functions [21]. The relative P_{50} values for membrane potential, proline transport and membrane permeability were 1:7.3:43, respectively, in the previous study and are 1:3.6:52, respectively, in this study. These values follow the same order and are of similar magnitudes. Variations in the magnitudes may result from differences in the experimental treatments; the wavelengths, intensities and the number of RB molecules per cell. The data available are not sufficient to identify the major variable.

In summary, these results indicate that radicals damage membrane functions more efficiently than $^1O_2^*$, even when both species are produced at the same locations in the plasma membrane. In addition, $^1O_2^*$ and radicals may initiate damage to some membrane components by a shared common mechanism and to other membrane components

by separate mechanisms. The results further indicate that when reactive radicals are produced, they are less selective than $^1O_2^*$ and that oxygen is involved in the damage mechanism for some membrane functions. Further work is required to determine whether the different pathways and effects in the plasma membrane that are initiated by two different types of reactive species will be reflected in subsequent cellular responses to photosensitization.

Acknowledgements

Support of this research by NIH grant RO1 GM30755 (I.E.K.), ONR contract N00014-94-I-0927 and FAPESP grant 93/1809-2 (A.C.T.) is gratefully acknowledged.

References

[1] Dougherty, T.J. (1993) Photochem. Photobiol. 58, 895–900.
[2] Henderson, B.W. and Dougherty, T.J. (1992) Photochem. Photobiol. 55, 145–157.
[3] Lui, H. and Anderson, R.R. (1992) Arch. Derm. 128, 1631–1636.
[4] Gunther, W., Searle, R. and Sieber, F. (1992) Semin. Hematol. 29, 88–94.
[5] North, J., Neyndorff, H. and Levy, J.G. (1993) J. Photochem. Photobiol. B Biol. 17, 99–108.
[6] Madison, R.D. and Macklis, J.D. (1993) Exp. Neurol. 121, 153–159.
[7] Macklis, J.D. (1993) J. Neurosci. 13, 3848–3863.
[8] Labrousse, A. and Satre, M. (1993) Photochem. Photobiol. 1993, 531–537.
[9] Labrousse, A., Bof, M. and Satre, M. (1993) J. Gen. Microbiol. 139, 841–845.
[10] Tarr, M. and Valenzeno, D.P. (1991) J. Mol. Cell. Cardiol. 23, 639–649.
[11] Tarr, M., Arriaga, E., Goertz, K.K. and Valenzeno, D.P. (1994) Free Rad. Biol. Med. 16, 477–484.
[12] Huang, A.J.W., Watson, B.D., Hernandez, E. and Tseng, S.C.G. (1988) Arch. Ophthalmol. 106, 680–685.
[13] Dietrich, W.D., Watson, B.D., Busto, R., Ginsberg, M.D. and Bethea, J.R. (1987) Acta Neuropathol. (Berlin) 72, 315–325.
[14] Liao, J.C., Roider, J. and Jay, D.G. (1994) Proc. Natl. Acad. Sci. USA 91, 2659–2663.
[15] Linden, K.G., Liao, J.C. and Jay, D.G. (1992) Biophys. J. 61, 956–962.
[16] Schmucker, D., Su, A.L., Beermann, A., Jackle, H. and Jay, D.G. (1994) Proc. Natl. Acad. Sci. USA 91, 2664–2668.
[17] Kanofsky, J.R. and Baker, A. (1993) Photochem. Photobiol. 57, 720–727.
[18] Kanofsky, J.R. (1991) Photochem. Photobiol. 53, 93–99.
[19] Specht, K.G. and Rodgers, M.A.J. (1990) Photochem. Photobiol. 51, 319–324.
[20] Specht, K.G. and Rodgers, M.A.J. (1991) Biochim. Biophys. Acta 1070, 60–68.
[21] Kochevar, I.E., Bouvier, J., Lynch, M. and Lin, C.-W. (1994) Biochim. Biophys. Acta 1196, 172–180.
[22] Dubbelman, T.M.A.R. and Van Steveninck, J. (1984) Biochim. Biophys. Acta 771, 201–207.
[23] Prinsze, C., Dubbelman, T.M.A.R. and Van Steveninck, J. (1990) Biochim. Biophys. Acta 1038, 152–157.
[24] Agarwal, M.L., Larkin, H.E., Zaidi, S.I.A., Mukhtar, H. and Oleinick, N.L. (1993) Cancer Res. 53, 5897–5902.
[25] Gibson, S.L., Murant, R.S. and Hilf, R. (1988) Cancer Res. 48, 3360–3366.
[26] Agarwal, M.L., Clay, M.E., Harvey, E.J., Evans, H.H., Antunez, A.R. and Oleinick, N.L. (1991) Cancer Res. 51, 5993–5996.
[27] Luna, M.C., Wong, S., Gomer C.J. (1994) Cancer Res. 54, 1374–1380.
[28] Allen, M.T., Lynch, M., Lagos, A., Redmond, R.W. and Kochevar, I.E. (1991) Biochim. Biophys. Acta 1075, 42–49.
[29] Krieg, M., Srichai, M.B. and Redmond, R.W. (1993) Biochim. Biophys. Acta 1151, 168–184.
[30] Fluhler, E.N., Hurley, J.K. and Kochevar, I.E. (1990) Biochim. Biophys. Acta 990, 269–275.